THE ASTROPHYSICAL JOURNAL, 275:391–404, 1983 December 1

A MEASUREMENT OF THE ENERGY SPECTRA AND RELATIVE ABUNDANCE OF THE COSMIC-RAY H AND He ISOTOPES OVER A BROAD ENERGY RANGE

W. R. WEBBER AND S. M. YUSHAK
Space Science Center, University of New Hampshire
Received 1983 February 14; accepted 1983 May 6

ABSTRACT

We have measured the spectra of the quartet of H and He isotopes over a wide range of energy at sunspot minimum modulation conditions in 1977. The measurements were made using balloon-borne and *Voyager* $dE/dx \times E$ telescopes. In both cases the isotopes are clearly resolved. The ^{3}He and ^{4}He observations provide a mutually consistent picture for the source spectra, galactic propagation, and solar modulation. The data define (1) interstellar ^{1}H and ^{4}He spectra of the form $dj/dT = CT^{0.3}\ (T + T_0)^{-0.3}$, where $T_0 = 0.3 \pm 0.1$ GeV per nucleon; (2) an interstellar matter path length for both ^{1}H and $^4\text{He} = 7.5 \pm 1$ g cm^{-2} below 1 GeV per nucleon; (3) a total residual modulation at the time of measurement that corresponds to a modulation parameter $\phi = 450 \pm 100$ MV. The ^{2}H observations suggest a very similar picture for galactic propagation. However, the measured ratios involving ^{2}H are consistent with those predicted for interstellar space rather than the ratio expected after solar modulation has been taken into account. This could be explained if energy loss in interplanetary space were small, since it is the energy loss effects that smooth and change the interstellar ratios. The ^{2}H results seem to be better explained by the now little used diffusion-convection solar modulation model. Rather than suggesting this as the correct explanation of the ^{2}H data, however, we feel that this is another indication of the inadequacy of the current modulation models. If energy loss in interplanetary space is small, then the ^{2}H measurements at $\sim$100 MeV per nucleon set an upper limit of matter traversed in interstellar space by ^{1}H of $\sim$15 g cm^{-2}. This is much less than required to explain the recent observations of cosmic-ray antiprotons at low energies.

Subject heading: cosmic rays: abundances

I. INTRODUCTION

The isotopes ^{2}H and ^{3}He in cosmic rays are generally believed to be of secondary origin, resulting mainly from the nuclear interactions of primary cosmic-ray protons and ^{4}He with the interstellar medium. As such, the H and He isotopes can be used as tracers to determine the mean matter path lengths of ^{1}H and ^{4}He in the interstellar medium and the energy spectra of these nuclei, particularly at low energies. Measurements of the ^{2}H/^{4}He and ^{3}He/^{4}He ratios at Earth can be used to deduce these quantities and also, as a result, to estimate the modulation parameter ϕ which gives a measure of the particle intensity reduction (solar modulation) in the heliosphere (e.g., Comstock, Hsieh, and Simpson 1972).

It is now generally accepted that the mean matter length for cosmic rays in the Galaxy as deduced from studies of heavier cosmic-ray nuclei such as C or Fe is $\sim$6 g cm^{-2} of hydrogen equivalent at energies $\lesssim$1 GeV per nucleon (e.g., Ormes and Freier 1978). Recent measurements appear to indicate a rather large cosmic-ray antiproton intensity at low energies (Buffington, Schindler, and Pennypacker 1981; Golden *et al.* 1979). These antiprotons would also be expected to be produced from nuclear interactions of protons in the interstellar medium (or in localized sources) and may indicate much larger path lengths, possibly up to $\sim$100 g cm^{-2}.

Measurements of the ^{2}H and ^{3}He abundances are relevant to this problem particularly those measurements made at sunspot minimum where the effects of solar modulation are smallest. Unfortunately, most previous measurements of these isotopes have been at energies $\lesssim$80 MeV per nucleon where the solar modulation affects are still large and where the presence of the anomalous He component complicates interpretation of the data.

In this paper we report measurements of these isotopes using two sets of detectors made during essentially the same minimum modulation period in 1977. One measurement was made with a balloon-borne telescope, the other with telescopes on board the *Voyager* spacecraft. Together they provide the widest energy range yet available for studying these isotopes: 14–150 MeV per nucleon for ^{2}H and 10–290 MeV per nucleon for ^{3}He.

II. INSTRUMENTATION AND FLIGHT DETAILS

a) Balloon Flight Instrument

This part of the data was obtained from a balloon-borne experiment flown from Fort Churchill, Canada, on 1977 July 4. The Mount Washington neutron monitor at the time of the flight was 2360—essentially at sunspot minimum conditions. The experiment remained at a float altitude of 2.9 g cm^{-2} for a total time of 32,400 s. Figure 1 shows a cross-sectional view of this instrument.

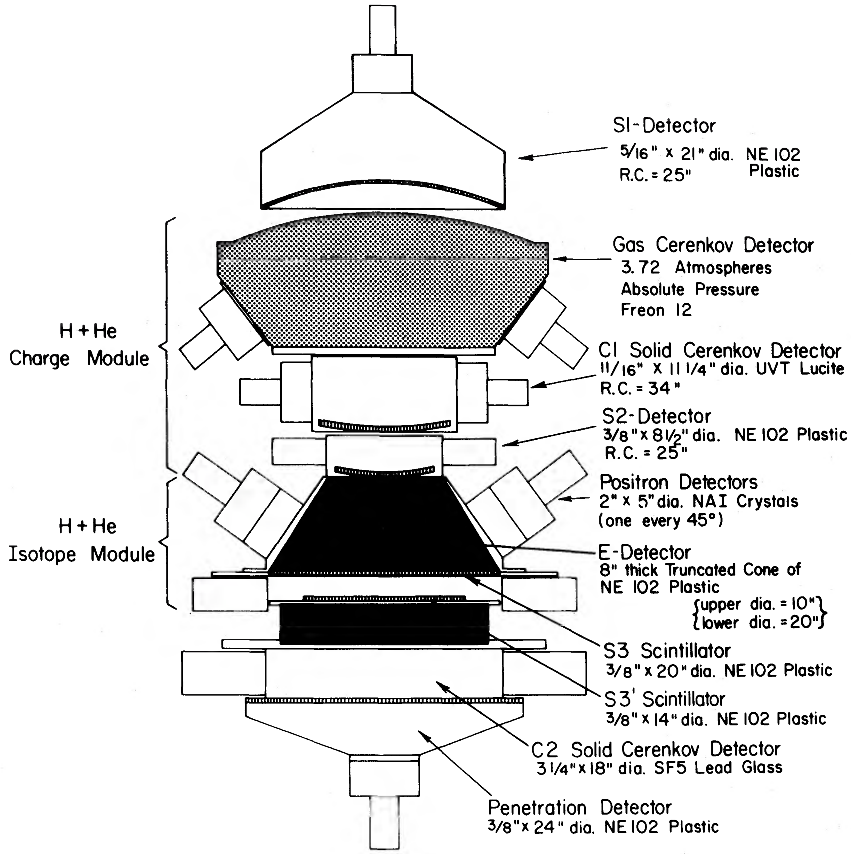

FIG. 1.—Schematic drawing of cosmic-ray telescope used to measure H and He isotopes on balloons

The energy spectra of the H and He isotopes were obtained over the energy range of interest using a double $dE/dx \times E$ measurement. The relevant counters were thin S1 and S2 scintillation counters providing the dE/dx measurement and a thick E1 counter for total energy measurement. The S3 scintillator was used to determine those particles that stop in E1. This telescope was also designed to measure electrons and positrons and, therefore, had several other detector elements. However, these were not relevant to the H and He isotope measurement.

The geometrical factor defined by the S1-S2 scintillator coincidence is 208 sr cm^2. The total payload weight was 200 kg. Twelve-bit pulse height analyzers were used on all detectors, and for an S1-S2 coincidence a data word of 260 bits was telemetered at a rate of 20 kb s^{-1} to a ground station. The data were recorded on magnetic tape which was then processed on a DEC-10 computer.

b) *Satellite Instrument*

The satellite instrument is part of an array of telescopes which comprised the cosmic-ray experiment aboard the *Voyager 1* and *2* spacecraft (Stone *et al.* 1977). The instrument used for these studies is designated the HET telescope and is shown schematically in Figure 2. This telescope is similar in principle to the one used on the balloon experiment, namely, a double $dE/dx \times E$ array. The telescope on *Voyager* is double-ended, and the data used here are from both the "thin" A end which uses two 150 μm thick solid-state detectors for the dE/dx measurement and the "thick" B end which utilizes two 2 mm thick Li drifted counters for the dE/dx measurement. The total energy measurement is made from the combined outputs of three thick Li drifted counters, with the last counter in the stack determining those particles that stop in the first three. Data were used from the *Voyager 1* spacecraft, which was launched in 1977 August. A 50 day quiet period between days 276 and 325 in 1977, when *Voyager* was still near the *Earth*, previously used for a study of the quiet time anomalous components (Webber, Stone, and Vogt 1979), was used for this study. The solar modulation, as evidenced by the Mount Washington neutron monitor rates, is almost identical to that at the time of the balloon flight 3 months earlier.

III. DATA ANALYSIS

The data analysis procedures for both experiments are very similar and can be described in a common manner. We have followed the usual procedure for the analysis of the data from cosmic-ray $dE/dx \times E$ telescopes. The first step is to place consistency criteria

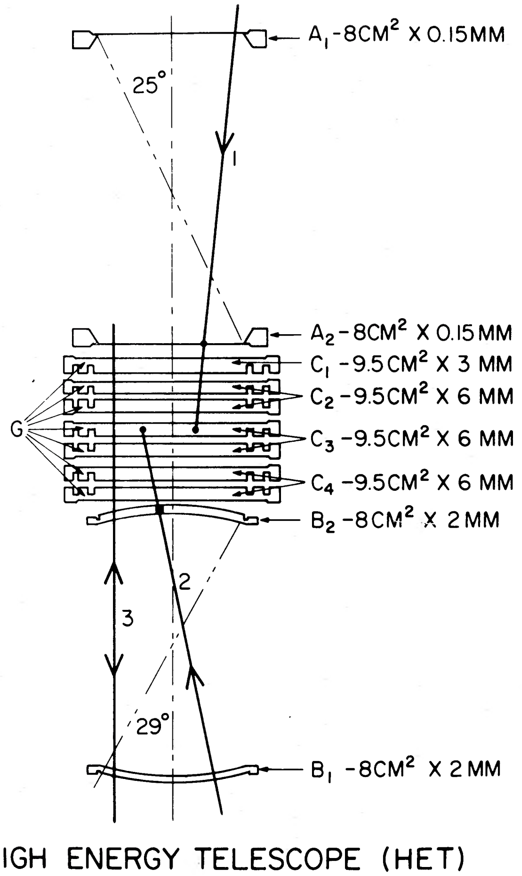

FIG. 2.—Schematic drawing of *Voyager* HET telescope

on the outputs of the two thin dE/dx counters to eliminate background events and events due to nuclear interactions. For each charge a matrix of the ratio of the two thin dE/dx counters versus E1 is formed. The dE/dx counter ratios are required to be consistent within $\pm 3\ \sigma$ with those expected for a given total E loss, where σ is a measure of the intrinsic fluctuations in the dE/dx signals. This criteria removes from 20%–40% of the total number of events but less than 1% of the valid noninteracting nuclei. Next a matrix using the combined dE/dx signals versus energy lost in E1 is formed, subject to the above selection criteria. These matrices are shown in Figures 3*a* and 3*b* for the balloon data and in Figure 4 for the *Voyager* data. The theoretical mass lines for the hydrogen and helium isotopes are shown on these matrices. They are obtained using a range-energy program and in-flight calibration data using the end-points of the various mass lines. For the balloon experiment, since the energy loss in the plastic scintillators is nonlinear, the nonlinearity was taken into account in constructing the mass lines.

It can be seen that the mass resolution in both telescopes is excellent, with the isotopes clearly resolved. Mass histograms for each set of isotopes may be constructed from these matrices by summing the number of events in pulse-height channel intervals which are parallel and equidistant from the mass lines. Mass histograms for the ^{1}He and ^{2}H isotopes from the *Voyager* data are shown in Figure 5 for several energy intervals. This is the most critical of the different mass histograms for H and He isotopes in the balloon and spacecraft data with regard to the separation of the isotopes, particularly at low energies.

IV. DETERMINATION OF THE ENERGY SPECTRA OF THE HYDROGEN AND HELIUM ISOTOPES

The determination of the energy spectra from *Voyager* data is straightforward because of the linearity of the system and the agreement between the predicted energy loss and the pulse-height channel calibration. The energy spectra for each species is determined by summing events in the various mass histograms and making a small correction for nuclear interactions in the telescope. The intensities are then obtained from the live time multiplied by a geometrical factor which is 1.61×10^6 s $\times\ 2 \times 1.6$ sr cm^2. This analysis is shown in tabular form in Table 1. The data are from the B telescope, except as indicated for ^{2}H and ^{3}He where A telescope data are also shown.

In spite of the stringent selection criteria, it is possible that background effects can be important, particularly for the low-energy ^{2}H spectrum. The principal source of this background is believed to be protons passing through the first element of either the A or B telescope at large angles outside the usual telescope opening angle and having a nuclear interaction in the Si from which a low-energy ^{2}H or ^{3}H particle is emitted within the opening angle of the telescope, thus producing an apparent "good" event. This type of background, if uncorrected, could be an important source of the unusual differences observed in earlier ^{2}H measurements (Meyer 1975). The correction is difficult to make theoretically since the appropriate cross sections and energy dependence of the emitted ^{2}H or ^{3}H nuclei are not well known for Si targets. Ramaty and Lingenfelter (1969) have discussed this problem for the production of ^{2}H and ^{3}H via the $p \rightarrow$ CNO reaction. Their calculations indicate that the production ratio of ^{2}H/^{3}H from such reactions should be ~ 4 at low energies.

Some ^{3}H is observed in both the balloon and the spacecraft data (see Figs. 3*a* and 4), and we have assumed that the ^{3}H observed in the *Voyager* data is a measure of the instrumental background since no cosmic-ray ^{3}H is to be expected. The relative abundance of ^{3}H and the mass resolution of ^{2}H and ^{3}H is shown in Figure 6, which includes all stopping nuclei from the B end telescopes. We have derived spectra for the ^{3}H nuclei from both the A end and B end telescopes, and these spectra are shown in Figure 7, along with the ^{2}H spectra. To correct the ^{2}H spectra we need to know the production ratio ^{2}H/^{3}H. As an independent check on the Ramaty and Lingenfelter (1969) calculations, we have determined the ^{3}H spectrum from the balloon data (see Fig. 8). These ^{3}H nuclei are all assumed to be atmospheric secondaries, and a comparison with the

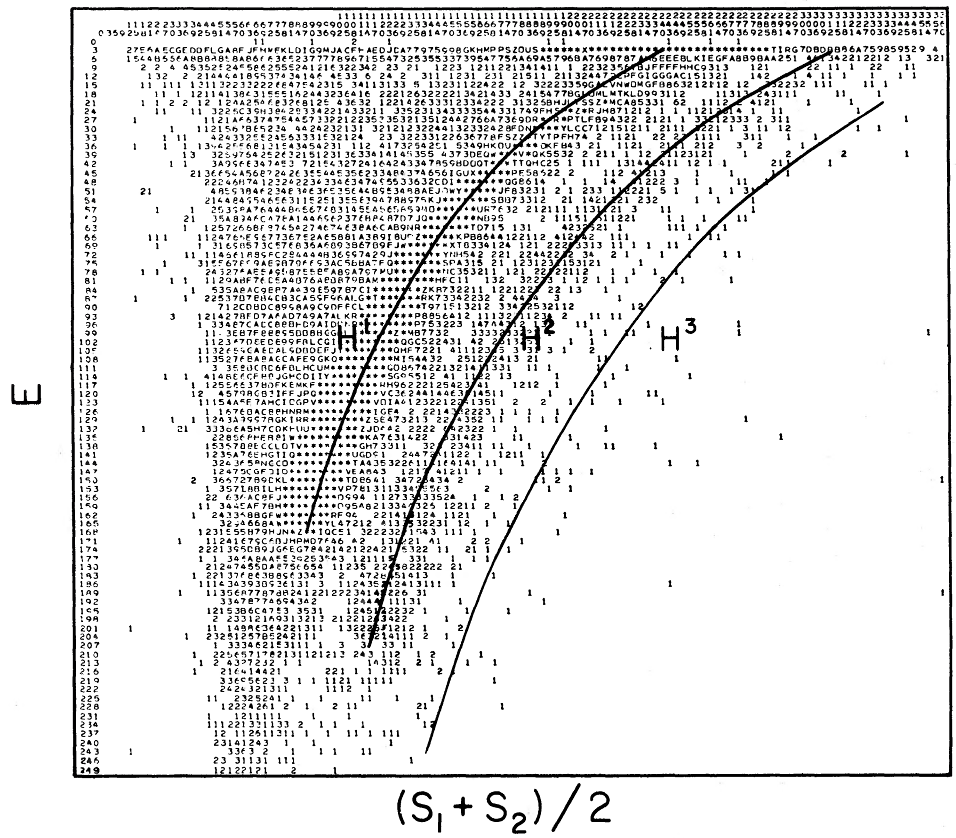

FIG. 3*a*

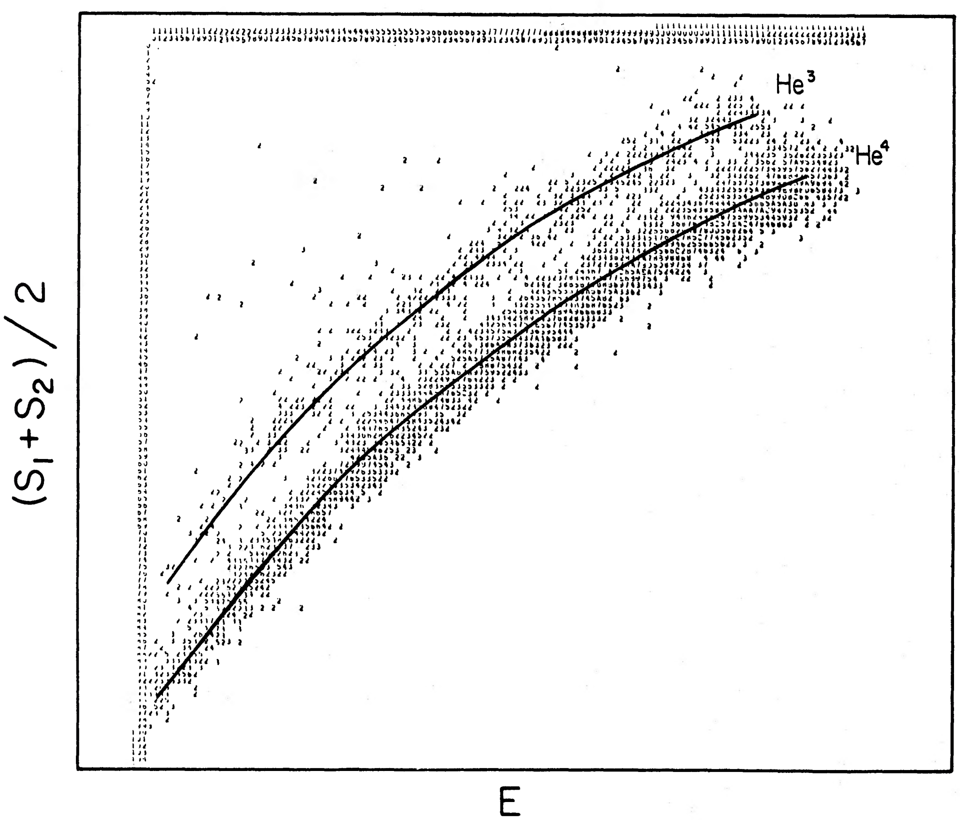

FIG. 3*b*

FIG. 3.—(*a*) Matrix showing $dE/dx \times E$ distribution for hydrogen events obtained with balloon telescope. (*b*) Matrix showing $dE/dx \times E$ distribution for helium events obtained with balloon telescope

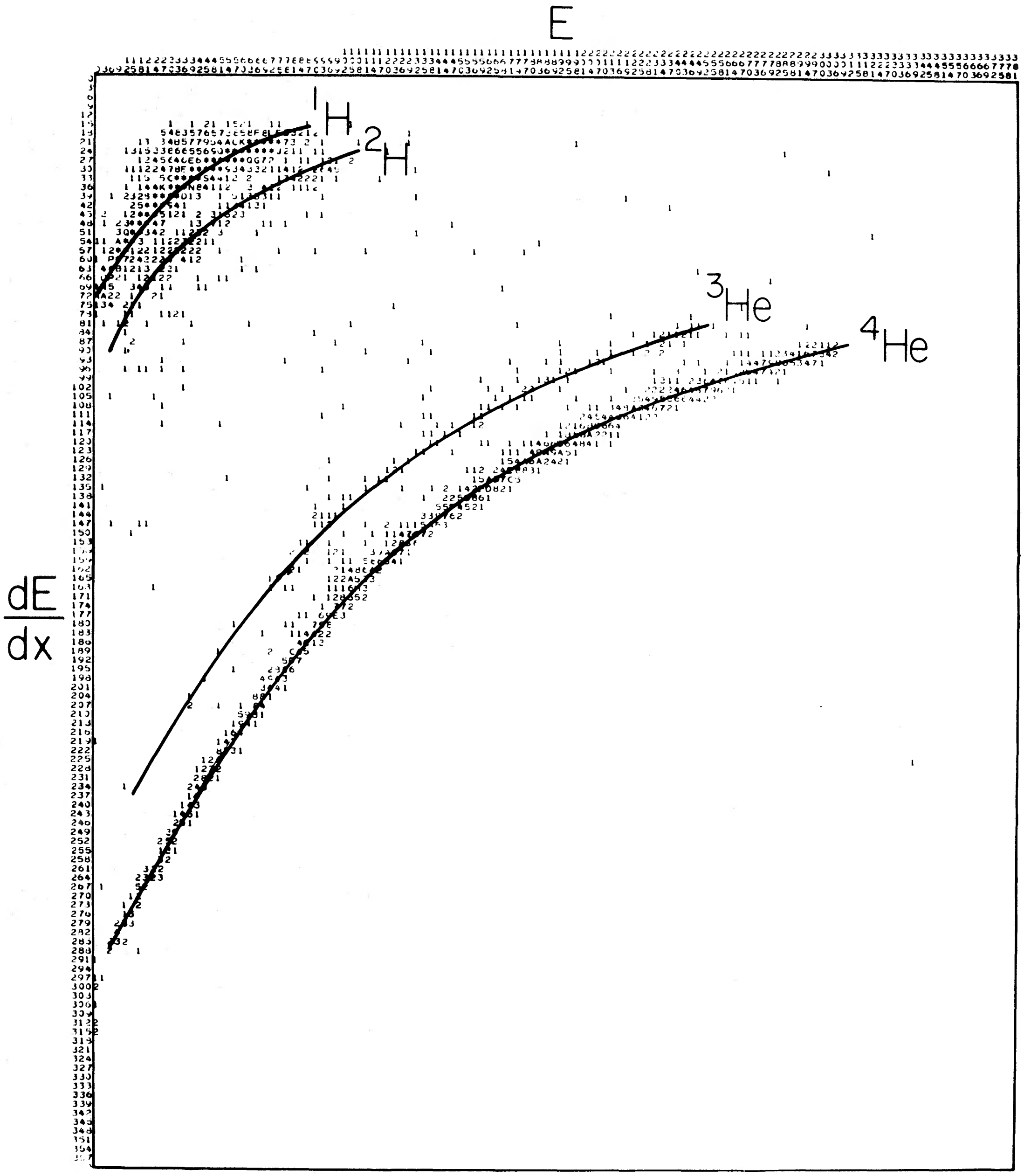

FIG. 4.—Matrix $dE/dx \times E$ distributions for hydrogen and helium events obtained with HET telescopes on *Voyager 1*

atmospheric ^{2}H intensity (see later discussion) provides a direct measure of the appropriate ^{2}H/^{3}H production ratio in air. This ratio, inferred from the balloon data, is 4 ± 1.

This ratio has been used along with the measured ^{3}H intensities to correct separately the ^{2}H spectra measured on *Voyager* by the A and B telescopes; the corrected spectra are shown in Figure 9. The correction amounts to $\sim 10\%$ at the highest *Voyager* energies and $\sim 50\%$ at 10 MeV per nucleon. These corrected spectra are used in all subsequent analysis.

The derivation of the spectra from the balloon data is more complex for several reasons. First of all, as we have noted, because of the nonlinearity between energy loss and light output in the plastic scintillators, the energy scale (essentially in the E-dimension) must be calibrated internally using the flight data. This is done using the minimum ionizing and endpoint channels for the various mass lines as observed in the different counters, together with the relationship

$$[(dL/dx)]_p = [A(dE/dx)_p]/[1 + K_1(dE/dx)_p]$$

TABLE 1

VOYAGER 1 PARTICLE INTENSITIES
(HET Telescopes; 1977 days 275–325)

Species	Energy (MeV per nucleon)	Events	$G\Delta t(\times 10^2)$	Particles $\left(\frac{\text{per m}^2\text{ sr s}}{\text{MeV per nucleon}}\right)$
^{1}H	63.8–69.0	729	1.19	1.14 ± 0.05
	55.5–63.8	971	1.45	0.88 ± 0.04
	49.1–55.5	814	1.64	0.79 ± 0.04
	41.6–49.1	956	1.86	0.68 ± 0.03
	34.2–41.6	990	2.04	0.64 ± 0.03
	27.0–34.2	821	2.17	0.51 ± 0.03
^{2}H	38.9–47.1	44	1.35	$(0.51 \pm 0.60) \times 10^{-2}$
	31.9–38.9	41	1.63	$(3.90 \pm 0.63) \times 10^{-2}$
	25.5–31.9	45	1.94	$(3.54 \pm 0.55) \times 10^{-2}$
	20.5–25.5	34	2.09	$(3.24 \pm 0.58) \times 10^{-2}$
	18.1–20.5	12	2.19	$(3.14 \pm 0.83) \times 10^{-2}$
^{2}H .... (A end)	25.2–38.1	59	1.36	$(3.66 \pm 0.53) \times 10^{-2}$
	17.4–25.2	45	1.61	$(3.60 \pm 0.58) \times 10^{-2}$
	11.6–17.4	31	1.88	$(2.81 \pm 0.49) \times 10^{-2}$
	6.8–11.6	23	2.08	$(2.46 \pm 0.50) \times 10^{-2}$
	3.2– 6.8	20	2.10	$(2.60 \times 0.58) \times 10^{-2}$
^{4}He	63.3–69.0	165	1.23	0.253 ± 0.020
	56.0–63.3	208	1.44	0.247 ± 0.016
	48.4–56.0	256	1.63	0.249 ± 0.014
	41.5–48.4	285	1.86	0.256 ± 0.013
	34.5–41.4	289	2.02	0.246 ± 0.013
	27.0–34.5	381	2.17	0.272 ± 0.013
^{3}He	66.2–88.0	38	1.32	$(2.07 \pm 0.32) \times 10^{-2}$
	52.2–66.2	37	1.64	$(1.79 \pm 0.29) \times 10^{-2}$
	39.1–52.2	39	2.02	$(1.45 \pm 0.27) \times 10^{-2}$
	33.1–39.1	12	2.17	$(0.96 \times 0.28) \times 10^{-2}$
^{3}He .... (A end)	49.0–65.6	28	1.33	$(1.45 \times 0.31) \times 10^{-2}$
	34.7–49.0	40	1.67	$(1.66 \times 0.26) \times 10^{-2}$
	21.6–34.7	18	2.04	$(0.75 \pm 0.19) \times 10^{-2}$
	7.6–21.6	21	2.10	$(0.74 \pm 0.18) \times 10^{-2}$

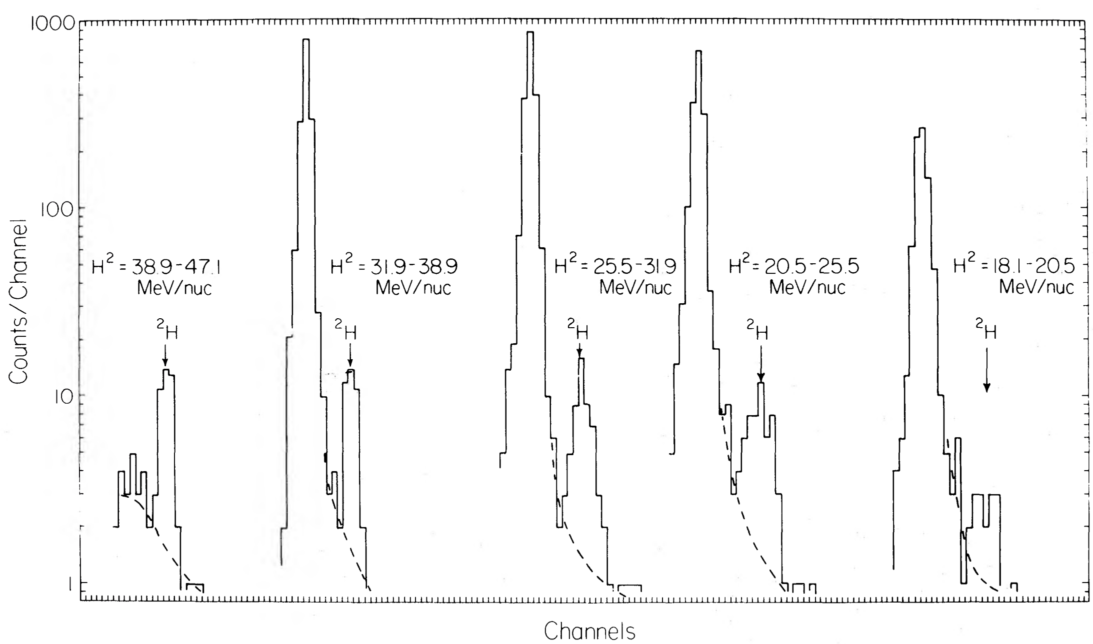

FIG. 5.—Mass histograms for H isotopes in several energy intervals obtained from the *Voyager 1* HET telescope data

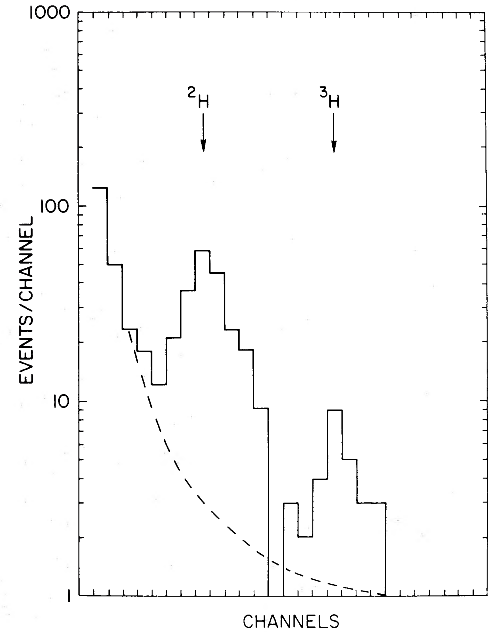

FIG. 6.—Mass histogram of stopping nuclei in *Voyager* B telescopes. Mass line centered on ^{2}H.

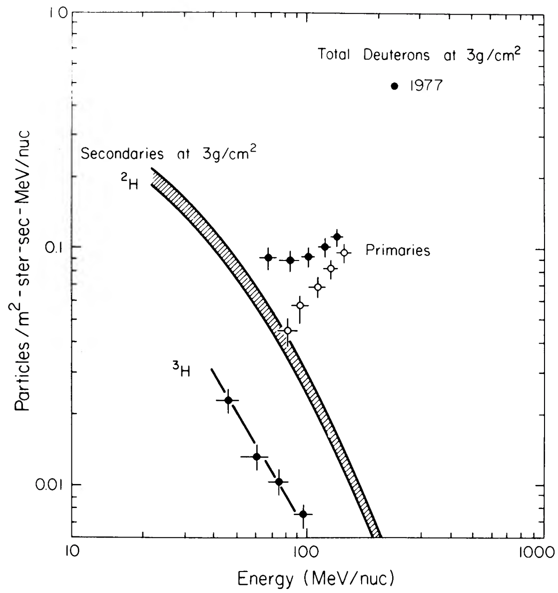

FIG. 8.—Comparison of the measured and predicted ^{2}H spectrum at an atmospheric depth of 3 g cm^{-2}. Also shown is ^{3}H spectrum.

to derive the values of dL/dx for the instrument. We find $K_1 = 0.018$ for H nuclei and $K_2 = 0.013$ for the He nuclei, in agreeement with what other workers find for NE 102 scintillator (e.g., Badhwar *et al.* 1967).

The events in the mass histograms are then summed and corrected for nuclear interactions to the top of the telescope (see Table 2). For the helium isotope data, the correction to the top of the atmosphere can be made directly since the secondary production is small. For both of the H isotopes an atmospheric secondary correction must be made, although it is minimized by

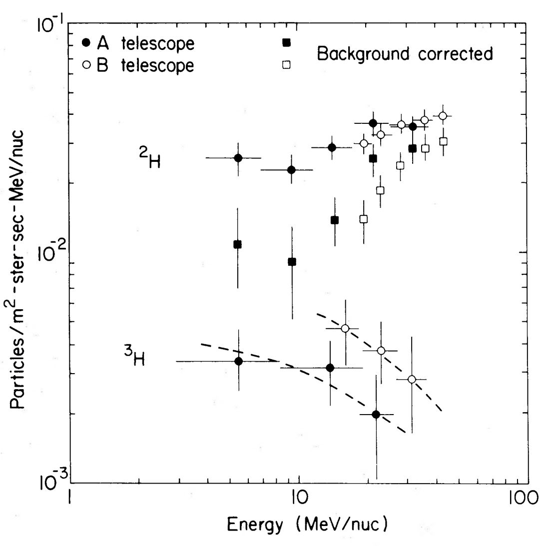

FIG. 7.—Spectra of ^{2}H and ^{3}H nuclei obtained from *Voyager* A and B telescopes. Corrected ^{2}H data are indicated.

the small floating depth of the balloon flight and the relatively high energies involved. In both cases this correction was made from a study of the growth of the secondary ^{1}H and ^{2}H components in several energy intervals in the atmosphere between 2.9 and 600 g cm^{-2}. A transport equation taking into account secondary production and losses due to ionization and nuclear interactions was used to fit the growth curve data (Yushak 1978). This secondary production is a more serious problem for ^{2}H than for ^{1}H, and in Figure 8 we show the secondary ^{2}H spectrum predicted at 2.9 g cm^{-2}, along with the measured deuteron intensity. The secondary intensity is greater than $\sim 50\%$ of the total intensity only in the lowest two energy intervals. The analysis of the balloon data and the correction to the top of the atmosphere is shown in Table 2 for H and He nuclei. The ^{1}H and ^{2}H spectra are shown in Figure 9, and the ^{3}He and ^{4}He spectra in Figure 10, along with the satellite data. Higher energy ^{1}H and ^{4}He spectra have also been obtained from the balloon flight data by unfolding the distribution of pulse heights in the Cerenkov detector, C1 (Webber and Yushak 1979). These spectra are shown for reference in Figures 9 and 10.

V. COMPARISON WITH OTHER MEASUREMENTS

There are no other ^{2}H and ^{3}He data reported for a time period similar to our measurements. The most recent data were obtained mainly at lower energies in 1972–1973. Solar modulation effects were somewhat greater in 1972–1973; e.g., the Mount Washington neutron monitor was typically 2300 in 1972–1973 versus 2360 at the time of our measurements. In general, the low-energy measurements of ^{2}H intensities by Teegarden

TABLE 2

BALLOON PARTICLE INTENSITIES
(1977 July 4)

Species	Energy (MeV per nucleon) at Top	Observed Events	Intensity at Top of Telescope[a]	Secondary Intensity[a]	Intensity at Top of Atmosphere[a]
$^1H + ^2H$	200–249	60,400	2.36	0.15	2.28 ± 0.12
	160–200	41,900	2.12	0.19	1.98 ± 0.13
	140–160	18,500	1.91	0.24	1.72 ± 0.12
	125–140	13,300	1.80	0.28	1.58 ± 0.10
	110–125	10,500	1.68	0.32	1.41 ± 0.09
$^3He + ^4He$	200–249	6430	0.318	...	0.341 ± 0.02
	160–200	4390	0.302	...	0.334 ± 0.02
	140–160	2960	0.298	...	0.320 ± 0.02
	125–140	1950	0.276	...	0.296 ± 0.02
	110–125	1525	0.259	...	0.278 ± 0.02
^2H	133–149	356	0.109	0.015	0.096 ± 0.08
	115–133	418	0.098	0.019	0.083 ± 0.07
	101–115	347	0.090	0.025	0.070 ± 0.06
	87–101	363	0.087	0.033	0.058 ± 0.06
	74– 87	360	0.086	0.045	0.045 ± 0.07
He	252–290	385	0.050	...	0.054 ± 0.04
	225–252	272	0.043	...	0.047 ± 0.04
	203–225	230	0.039	...	0.042 ± 0.04
	183–203	210	0.036	...	0.038 ± 0.04
	161–183	198	0.030	...	0.033 ± 0.04

[a] Intensities in particles m^{-2} sr^{-1} s^{-1} MeV per nucleon ($G\Delta t = 674$ m^2 sr s). The principal corrections are for nuclear interactions in the telescope and in the atmosphere. The interaction mean free paths for the telescope, consisting mostly of plastic (CH), used in the calculations are $^1H = 75$ g cm^{-2}, $^2H = ^3He = ^4He = 35$ g cm^{-2}. For air, the mean free paths are taken to be 1.3 times those in CH.

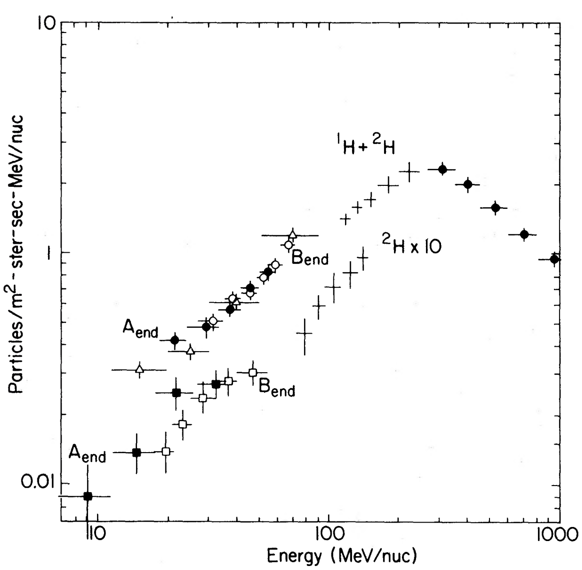

FIG. 9

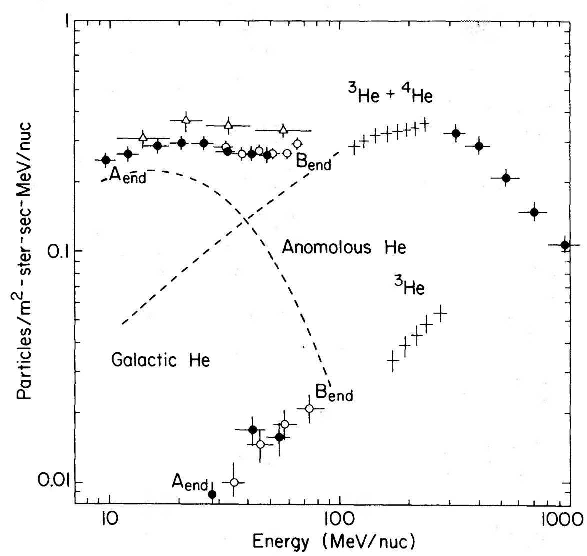

FIG. 10

FIG. 9.—Spectra of ^1H and ^2H nuclei obtained from the balloon and spacecraft experiments. Data points designated by -Δ- are from Bastian *et al.* (1979), for a similar time period.

FIG. 10.—Spectra of ^3He and ^4He nuclei obtained from the balloon and spacecraft experiments. Estimated magnitudes of the anomalous He component and galactic He are shown by dashed lines at low energies. Data points designated by -Δ- are from Bastian *et al.* (1979), for a similar time period.

et al. (1975) and Mewaldt, Stone, and Vogt (1976) made in 1972–1973 lie a factor ~ 1.5–2 below our measurement, and the ^{3}He intensities measured by Garcia-Munoz, Mason, and Simpson (1975), Mewaldt *et al.* and Webber and Schofield (1975) made in 1972–1973 are also a factor of 1.5–2 below our low-energy data points. We believe that these differences can be explained by the reduced solar modulation at the time of our measurements, this effect also being present in the higher energy ^{1}H and ^{4}He intensities which are significantly larger than those measured in 1972–1973.

Proton and ^{4}He intensities measured on *IMP 8* by Bastian *et al.* (1979) during late 1977 and early 1978 are shown as a reference in Figures 9 and 10. Note that in all the measurements shown in these two figures, $^4\mathrm{He} = {}^3\mathrm{He} + {}^4\mathrm{He}$ and $^1\mathrm{H} = {}^1\mathrm{H} + {}^2\mathrm{H}$.

VI. INTERPRETATION OF THE DATA: GENERAL

In the interpretation of the data the absolute values of the intensities of all the components are important. Also very useful in the analysis are the ^{3}He/^{4}He, ^{2}H/^{4}He, and ^{2}H/^{3}He ratios. These various ratios are shown in Figures 11 and 12, along with predictions based on interstellar propagation models and solar modulation effects to be discussed later. It should be noted that the low energy ^{4}He spectrum below ~ 80 MeV per nucleon is influenced by an additional component known as anomalous ^{4}He. This component results in a much flatter total ^{4}He spectrum than would occur if only modulation of a simple interstellar component was present. The origin of the anomalous ^{4}He and other anomalous charges such as N and O is presently uncertain, and from the point of view of the analysis in this paper this will significantly affect the ratios where ^{4}He is involved below ~ 80 MeV per nucleon. The division of the total ^{4}He into these two components is shown in Figure 10 where the galactic ^{4}He is obtained below 80 MeV per nucleon by fitting the total ^{4}He above 100 MeV per nucleon to a modulation parameter $\phi = 400$ MV (see later discussion).

In the interpretation of the data it is necessary to have predictions of the expected ^{2}H and ^{3}He intensities in interstellar space outside of the solar modulation region. These predictions are based on a particular model for interstellar propagation, along with an accounting of all the fragmentation cross sections for ^{1}H and ^{4}He on interstellar ^{1}H and ^{4}He that lead to the production of ^{2}H and ^{3}He. This is a formidable calculation, and we have used the results of propagation calculations of Meyer (1974) and Ramadurai and Biswas (1974). Each of these authors has used essentially the same propagation model and derives very similar ^{2}H and ^{3}He spectra for a given set of ^{1}H and ^{4}He input spectra. From a comparison of their results and a consideration of the uncertainties in the fragmentation cross sections it appears that the overall systematic errors in the predicted ^{2}H and ^{3}He intensities for a given set of propagation parameters are $\sim \pm 10\%$.

For the propagation calculations it is assumed that the leaky box model for cosmic-ray propagation and escape from the Galaxy applies. This results in an exponential distribution of matter path lengths traversed by the cosmic rays with a characteristic value λ_{esc}. As we have noted earlier, the application of this model to a wide variety of heavier nucleon data leads to an average matter path length $\lambda_{\text{esc}} = 6 \pm 1$ g cm^2 of hydrogen traversed below ~ 1 GeV per nucleon (e.g., Ormes and Frier 1978). Above 1 GeV per nucleon this

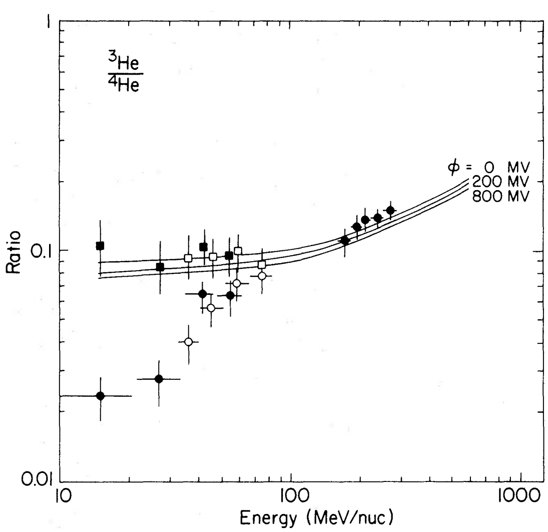

FIG. 11*a*

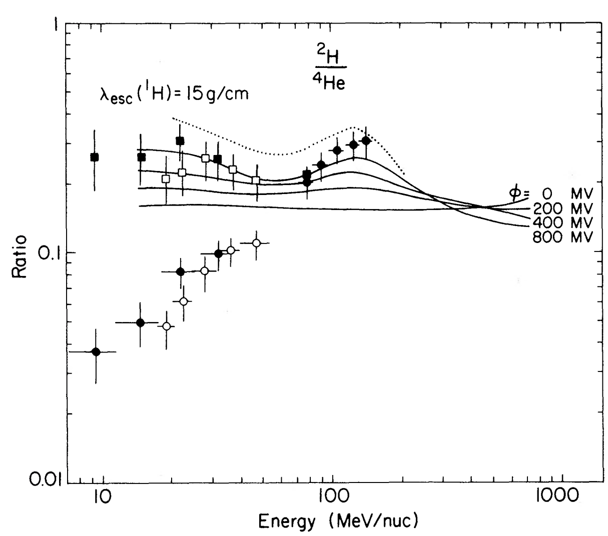

FIG. 11*b*

FIG. 11.—(*a*) The ^{3}He/^{4}He ratios measured as a function of energy in this experiment. Predictions of interstellar propagation model for ^{1}H and ^{4}He spectra with $T_0 = 0.4$ MeV per nucleon and $\lambda_{\text{esc}} = 7.5$ g cm^{-2} and for various values of the modulation parameter ϕ (as discussed in text) are shown as solid lines. Corrections to the ^{3}He/^{4}He ratios for the presence of anomalous ^{4}He at low energies are shown by open and solid squares. (*b*) Measured ^{2}H/^{4}He ratios at low energies and predictions based on same interstellar propagation and local modulation as for He. Ratios corrected for anomalous ^{4}He are shown by open and solid squares at low energies.

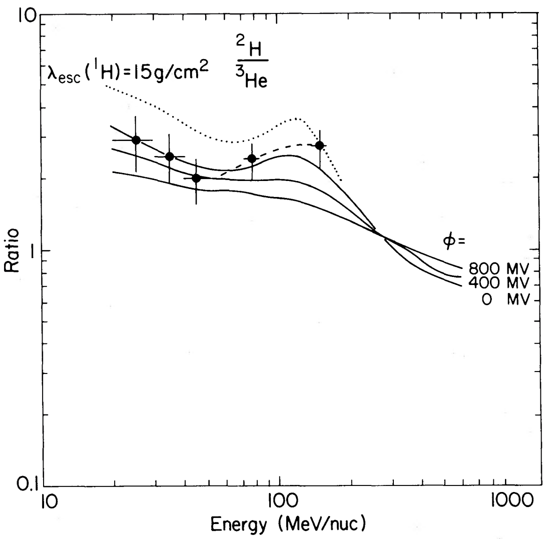

FIG. 12.—The $^2H/^3He$ ratio measured in this experiment. The interstellar ratio predicted on the basis of the propagation parameters used to explain the He isotopes is shown as $\phi = 0$. The effects of solar modulation are shown, as is the effect of increasing the ^1H path length to 15 g cm^{-2}.

path length appears to decrease slowly with energy (e.g., $\sim T^{-0.5}$). This decreasing path length has not been taken into account in the work of Meyer (1974) and Ramadauri and Biswas (1974). It will be a relatively small effect at the low energies we are considering here, however.

The total amount of ^2H and ^3He production depends strongly on the mean matter path length and also on the shape of the interstellar ^1H and ^4He spectra. We have considered interstellar spectra of the form $dJ/dT = CT^{0.3}\ (T + T_0)^{-3.0}$, a form that closely approximates the forms used by the above authors. Here C is a normalizing constant, T is the kinetic energy in GeV per nucleon, and T_0 is a variable parameter which takes on values between zero and 0.94 GeV per nucleon. For $T_0 = 0$ the local interstellar spectrum is a power law in kinetic energy, while for $T_0 = 0.94$ GeV per nucleon, a power law in total energy is obtained. Note also that the assumed spectra asymptotically approach a spectral index equal to -2.7 at high energies, in agreement with measurements.

VII. HELIUM ISOTOPE DATA

We consider the He isotope data first since they appear to have a more direct interpretation and since ^3He is produced principally by only ^4He. It is desirable to separate, as cleanly as possible, the effects of solar modulation and interstellar propagation. This may be done by simultaneously studying the $^3He/^4He$ ratio, which depends mainly on the amount of interstellar production (e.g., λ_{esc}), and the absolute intensities of these components, which depend strongly on solar modulation as well. For example, the ^4He intensity at Earth will be a function of only the interstellar ^4He spectrum and the amount of solar modulation. The first step in our analysis is, therefore, to reproduce the ^4He observations seen at Earth. To do this we modulate the various possible interstellar spectra by solving the full Fokker-Planck transport equation, including the effects of diffusion, convection, and adiabatic deceleration in the interplanetary medium (e.g., Gleeson and Axford 1968). The modulation parameter we use is defined as

$$\phi = \tfrac{1}{3}\int V dr/K(r)\,,$$

where V is the solar wind speed and $K(r)$ is the radial dependence of the diffusion coefficient, here taken to be independent of r (Gleeson and Urch 1971). The rigidity dependence of K is taken to be $\sim\beta P$ above 1 GV rigidity, and $\sim\beta$ below 1 GV.

This is the conventional modulation model used by most observers to calculate numerically the effects of solar modulation. Recent observations show that this is only an approximation to the dynamic modulation that is actually occurring (e.g., McDonald *et al.* 1981; Webber and Lockwood 1981). It is, however, the only model presently available that leads to simple numerical predictions that can be compared with observations. We should also note that because of adiabatic deceleration in this model the particles may lose up to ~ 200 MeV per nucleon in the interplanetary medium; thus, particles observed at a low energy at Earth comes from a population of higher energies in the interstellar medium. In effect, the higher the energy at Earth, the smaller the fraction of energy lost in the interplanetary medium. This illustrates the importance of extending the measurements to higher energies.

In Figure 13 we show sample interstellar ^4He spectra calculated for various values of T_0. For each of these spectra a value of the modulation parameter ϕ can be found that will reproduce the observed ^4He intensity at an energy of 200 MeV per nucleon. Similar values of ϕ are obtained for other energies. One sees that the parameter T_0 varies inversely with ϕ; i.e., for small values of T_0, the magnitude of the interstellar ^4He spectrum is large, and, therefore, a larger value of the modulation parameter is required to reduce the interstellar spectrum to that observed at Earth.

The next step in our analysis is to follow a similar procedure for ^3He. We need to obtain the local interstellar ^3He spectrum for any given ^4He spectrum and for various values of the matter path length λ_{esc}. To do this we use primarily the propagation calculations of Meyer (1974) which cover a wide range of input spectra and values of λ_{esc}. The calculated interstellar ^3He spectra can then be modulated to fit the ^3He observations at Earth, and a relationship between T_0 and ϕ for each value of λ_{esc} can be obtained. This relationship is shown in Figure 14 for $\lambda_{esc} = 4$, 6, and 8 g cm^{-2}, also at an energy of 200 MeV per nucleon. The obvious requirement that the sets of T_0 and ϕ be the same when derived from either the ^3He or the ^4He data defines the value of λ_{esc} to be between 7 and 8 g cm^{-2}, with an error of $\sim 10\%$ due to the fragmentation cross sections.

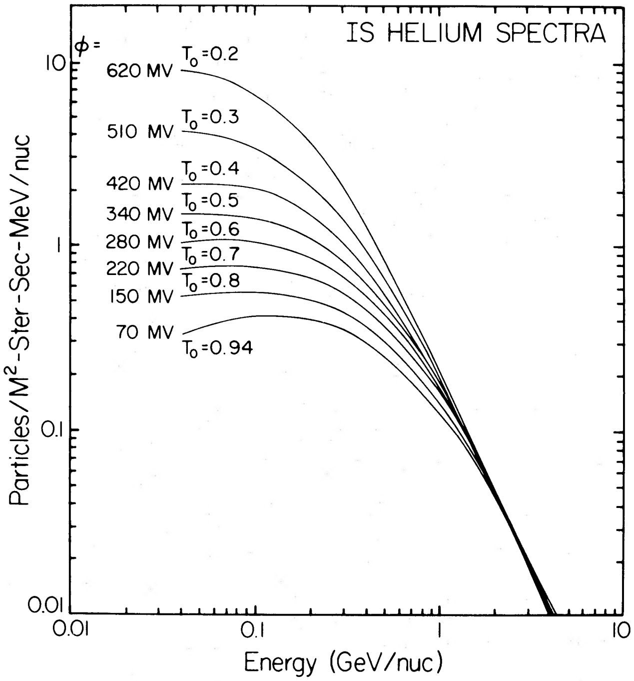

FIG. 13.—Interstellar ^{4}He spectra obtained for various values of T_0. Values of ϕ necessary to reproduce ^{4}He spectrum observed at Earth are also shown.

The next step in our analysis is to utilize the ^{3}He/^{4}He abundance ratio measurements. Note first that above ~ 100 MeV per nucleon, the ^{3}He/^{4}He ratio is essentially independent of ϕ. The principal influence on the ^{3}He/^{4}He ratio is, therefore, the value of the interstellar path length λ_{esc} as expected. If we now use the value of $\lambda_{esc} = 7$–8 g cm^{-2} derived from the considerations in Figure 14 and the fact that the ^{3}He/^{4}He ratio does not depend strongly on ϕ, we may set limits on the parameter T_0 using the measured ^{3}He/^{4}He ratio. This is done as follows: Figure 15 shows the variation of T_0 with λ_{esc} for various values of the interstellar ^{3}He/^{4}He ratio. The measured value of this ratio near Earth is 0.126 ± 0.015 at 200 MeV per nucleon. The corresponding interstellar ratio from Figure 11*b* is 0.135 ± 0.015 at 200 MeV per nucleon. Thus, the interstellar ^{3}He/^{4}He ratio must have a value that lies between ~ 0.12 and 0.15, and for values of λ_{esc} between 7 and 8 g cm^{-2} we see from the cross-hatched area in Figure 15 that T_0 is required to have values between ~ 0.20 and 0.45 GeV per nucleon. It can be seen from Figure 14 that for this range of values for the parameter T_0 the required values for the residual modulation parameter ϕ lie between 400 and 650 MV. Finally, in Figure 16, we show the interstellar ^{3}He and ^{4}He spectra obtained using $T_0 = 0.40$ GeV per nucleon, the modulated spectra obtained from these interstellar spectra using $\phi = 400$ MV and the observations.

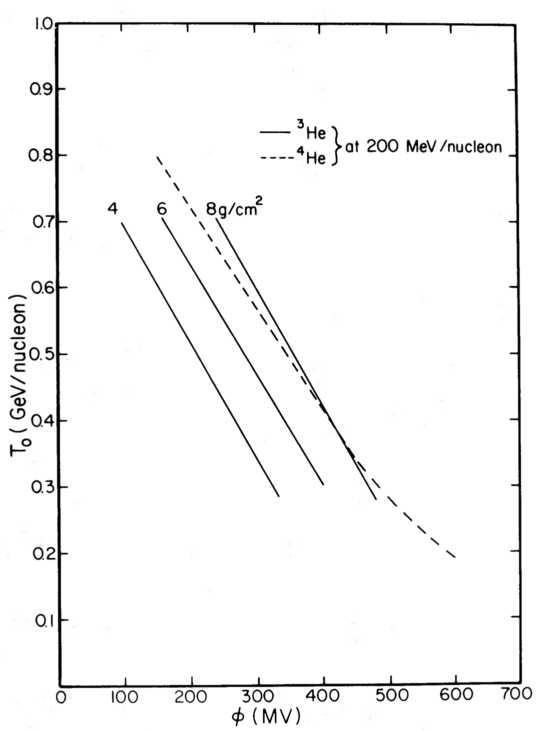

FIG. 14

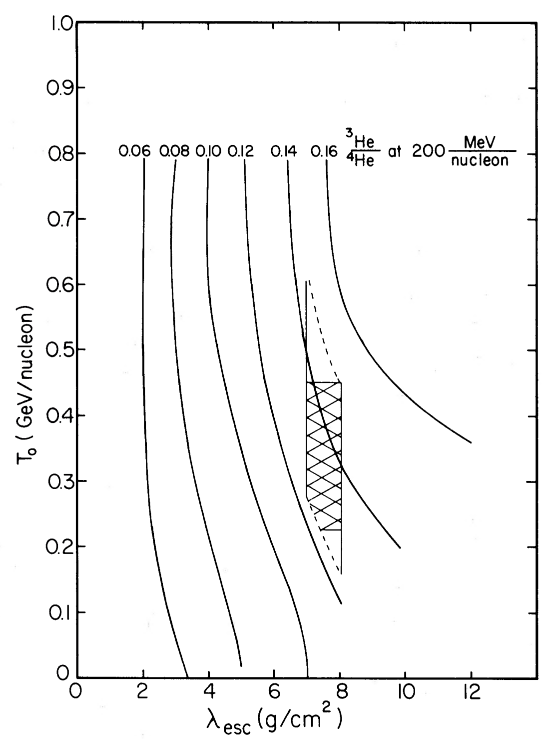

FIG. 15

FIG. 14.—Relationship between T_0 and the modulation parameter ϕ required to produce the observed ^{4}He intensity at 200 MeV per nucleon at Earth. Similar relationships required to produce ^{3}He intensity at 200 MeV per nucleon at Earth are also shown for several values of λ_{esc}.

FIG. 15.—Variations of the interstellar ^{3}He/^{4}He ratio at 200 MeV per nucleon as a function of the mean interstellar path length λ_{esc} and the spectral parameter T_0. Observational limits indicated by cross-hatched area.

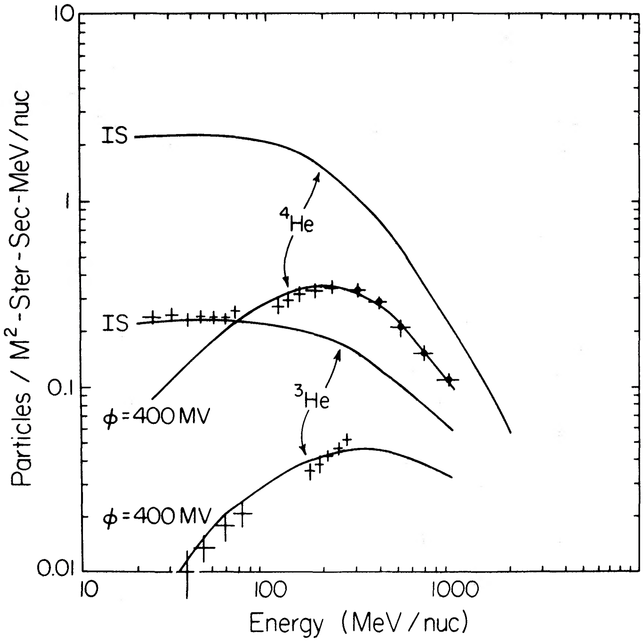

FIG. 16.—The interstellar ^{3}He and ^{4}He spectra obtained using a spectral parameter $T_0 = 0.4$ GeV per nucleon and the spectra modulated with $\phi = 400$ MV. Observations made in this experiment are also shown.

Basically, we have shown that a mutally consistent picture of galactic propagation and solar modulation can be obtained with those new ^{3}He and ^{4}He data. The mean amount of matter tranversed by ^{4}He is 7.5 g cm^{-2}, with an error of $\sim 10\%$. This is consistent with the matter traversal of 6 ± 1 g cm^{-2} obtained at energies $\lesssim 1$ GeV per nucleon obtained from a study of the fragmentation of heavier cosmic-ray nuclei.

VIII. HYDROGEN ISOTOPE DATA

The ^{2}H observations reported here are unique for two reasons: (1) they cover the widest energy range for this isotope yet studied; and (2) a relatively high flux of deuterons is observed at ~ 150 MeV per nucleon (almost 10% of the proton flux). The ^{2}H results do not admit of such a simple and clean interpretation as the helium isotopes, however, possibly because a significant component of ^{2}H flux is due to proton interactions in interstellar space.

The ^{2}H spectrum has been presented in Figure 9, the ^{2}H/^{4}He ratio in Figure 11*b*, and the ^{2}H/^{3}He ratio in Figure 12. In order to compare these results with predictions we have used the parameters derived from the analysis using the He isotopes, that is, $T_0 = 0.4$ GeV per nucleon and $\phi = 400$ MV. Shown in Figure 17 are the estimated interstellar ^{1}H and ^{2}H spectra and those calculated at 1 AU, along with the observations. There are several interesting aspects of the ^{2}H data summarized in Figures 11, 12, and 17. Consider the ^{2}H/^{4}He ratio in Figure 11*b*. This ratio, when corrected for the presence of anomalous ^{4}He at low energies, shows evidence of a minimum at ~ 60 MeV per nucleon, with an increase at both lower and higher energies. The increase at lower energies arises because of the correction of the ^{4}He spectrum for the anomalous He and is uncertain; however, the ^{2}H/^{3}He ratio should be free from this correction and also exhibits a similar behavior. This supports the details of the anomalous He correction and suggests that this increase is real.

Note that the ^{2}H/^{4}He and ^{2}H/^{3}He ratios as corrected in this manner agree well with the predictions to be expected using the interstellar propagation parameters derived from He and for a modulation parameter $\phi = 0$. This does not mean that the modulation itself is zero, since obvious modulation effects are apparent in Figure 17. Figures 11*b* and 12 illustrate the effect solar modulation has on these ratios. As noted earlier, it has only a small effect on the ^{3}He/^{4}He ratio, but it has a much larger effect on the ^{2}H/^{4}He ratio, and hence, also on the ^{2}H/^{3}He ratio. In effect, the ratios involving ^{2}H are reduced as the solar modulation increases and the distinct variations in the ratios calculated for the interstellar spectra are smoothed out. At the time of our measurement, ϕ, as deduced from the He data, is at least 400 MV; therefore, the observed ^{2}H ratios, as well as the ^{2}H intensity (Fig. 17), are greater than the predictions.

The smoothing effect of the solar modulation basically arises because of the interplanetary energy loss which redistributes the particles at a lower energy than they

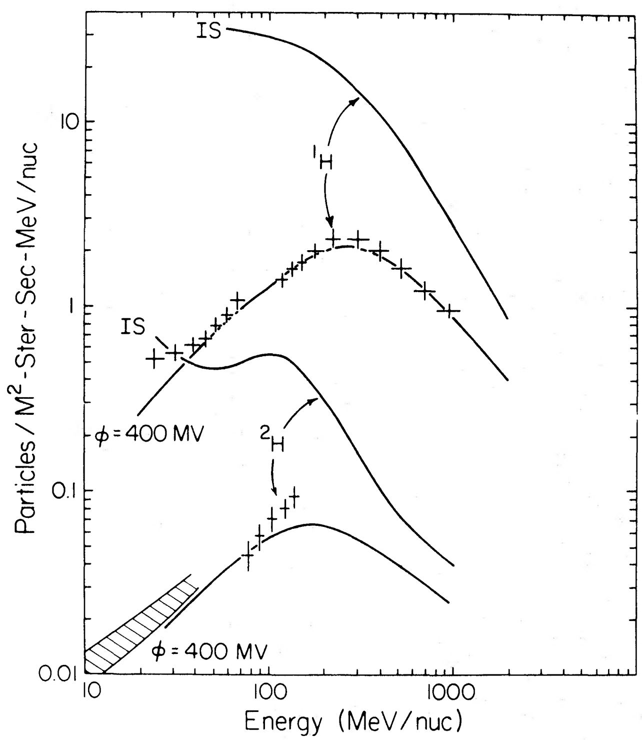

FIG. 17.—The interstellar ^{1}H and ^{2}H spectra obtained using a spectral parameter $T_0 = 0.4$ GeV per nucleon and the spectra modulated with $\phi = 400$ MV. Observations made in this experiment are also shown.

had in interstellar space. The energy loss term in the transport equations has been discussed at some length (see, e.g., Goldstein, Fisk, and Ramaty 1970; Urch and Gleeson 1972; Meyer 1975; McDonald *et al.* 1977). It has been difficult to verify experimentally that the predicted energy loss effects exist, although both the $j \approx T$ spectral shape observed at lower energies and the charge splitting of the modulation of H and He have been suggested as indicating the presence of energy loss (see, e.g., Lezniak and Webber 1971; Rygg and Earl 1971; Gleeson 1972).

This difficulty is due in part to the featureless nature of most of the interstellar spectra. It has been suggested that one test of energy loss effects would be to examine how a spectral feature at a particular energy in the interstellar spectrum might be distorted or transformed to a lower energy at 1 AU by these effects. The most pronounced feature in any of the interstellar spectra apparently exists for the ^{2}H spectrum at ~ 100 MeV per nucleon. This arises from the reaction of cosmic-ray ^{1}H on interstellar ^{1}H producing $^2\mathrm{H} + \pi^+$ and, therefore, is also an independent indicator of the amount of matter cosmic-ray ^{1}H has traversed.

If energy loss is neglected in the transport equations, one has the well-known simple diffusion-convection model that was used until the late 1960s to interpret the modulation of cosmic-ray protons and helium nuclei (e.g., Ormes and Webber 1968; Hsieh 1970). In this model any interstellar spectral features will be preserved at the same energy, and, therefore, these features will appear in the various charge ratios as well. In addition, the rigidity dependence of the modulation as illustrated in Figures 16 and 17 will be different than in the models in which energy loss is important and, in fact, will depend specifically on the energy or rigidity dependence of the diffusion coefficient itself. In essence, the observations involving the ^{2}H ratio, as well as the ^{2}H spectrum, can be reproduced better using a simple diffusion-convection model than the more commonly used transport equations which contain energy loss. We should note here that recently McDonald (1980) has suggested that the proton and helium nuclei modulation and radial gradient data obtained from the *Pioneer 10* and *11* spacecraft can be explained better using a simple diffusion-convection model. Also, the puzzling behavior of the $^2\mathrm{H}/^4\mathrm{He}$ ratio observed throughout the recent modulation cycle has been discussed by Meyer (1975), who suggested that the interplanetary deceleration was small during part of the solar cycle. Our measurements again bring into focus the modulation problem and reinforce the considerable body of data that does not appear to be consistent with the commonly used modulation models. We believe that to pursue this question further is beyond the scope of the paper, but it is a point we intend to explore.

An important by-product of this discussion is related to the production of ^{2}H by cosmic-ray ^{1}H in interstellar space. Approximately 30% of all ^{2}H at ~ 100 MeV is produced by cosmic-ray ^{1}H through the reaction discussed earlier, and at lower energies this fraction increases to $\sim 50\%$ as a result of cosmic-ray ^{1}H interactions with interstellar He. All of these secondary deuterons are produced by relatively high energy cosmic-ray protons and are, therefore, not strongly dependent on the shape of the low-energy interstellar ^{1}H spectrum. These are the same cosmic-ray protons that may produce the antiprotons that have been recently observed (Golden *et al.* 1979; Buffington, Schindler, and Pennypacker 1981). A possible explanation of these high antiproton intensities is the passage of cosmic-ray protons through considerably more matter than the commonly assumed 6–8 g cm^{-2} deduced for He and heavier nuclei. If these protons were to have passed through 2 times as much matter as the He data indicate, the predicted interstellar $^2\mathrm{H}/^4\mathrm{He}$ and $^2\mathrm{H}/^3\mathrm{He}$ ratios would be increased as indicated in Figures 11 and 12. Any increase beyond this in the ^{2}H production would be inconsistent with our measured $^2\mathrm{H}/^4\mathrm{He}$ and $^2\mathrm{H}/^3\mathrm{He}$ ratios if interplanetary energy loss is unimportant; therefore, subject to this assumption, we can set an upper limit to the matter length traversed by cosmic-ray ^{1}H of ~ 15 g cm^{-2}. This matter limit also places severe limits on the "old" component in the closed galaxy model of Peters and Westergaard (1977). If interplanetary energy loss is present as predicted in most models, then these effects will not be observable at 1 AU.

IX. SUMMARY AND CONCLUSIONS

We have measured the spectra of the quartet of H and He isotopes over a wide range of energy at sunspot minimum modulation conditions. The measurements were made using a combination of balloon-borne and spacecraft $dE/dx \times E$ telescopes. In both cases, excellent mass resolution is obtained so that the isotopes are unambiguously resolved. The simultaneous helium isotope observations are used to provide a mutually consistent picture of galactic propagation and solar modulation. The data define (1) interstellar ^{1}H and ^{4}He spectra in the form $dj/dT = CT^{0.3}\,(T + T_0)^{-0.3}$, where $T_0 = 0.30 \pm 0.1$ GeV per nucleon; (2) an interstellar matter path length for both ^{1}H and $^4\mathrm{He} = 7.5 \pm 1$ g cm^{-2} below 1 GeV per nucleon; (3) a total residual modulation for ^{4}He of about a factor of 10 at 100 MeV per nucleon at the time of measurement in 1977. This corresponds to a residual modulation parameter $\phi = 450 \pm 100$ MV at this time.

The ^{2}H observations suggest a very similar picture for the galactic propagation of ^{1}H and ^{4}He. However, the ratios involving ^{2}H seem to fit better the predictions for $\phi = 0$, rather than the predicted ratios after solar modulation has been taken into account. This could be explained if energy loss in interplanetary space were unimportant, since it is the energy loss effects that smooth and change the interstellar ratios. If energy loss is neglected, one returns to the well-known simple diffusion-convection model used in the past to explain the overall cosmic-ray modulation. Rather than suggesting that this is a correct solar modulation model, we feel that this is just another indication of the inadequacy of the current modulation models used to explain the 11 yr variation.

If energy loss in interplanetary space is small, then the ^{2}H measurements at energies ~ 100 MeV per nucleon or less give important information on the amount of interstellar matter tranversed by cosmic-ray ^{1}H. Subject to this assumption, this limit is ~ 15 g cm^{-2}, which is much less than required to explain recent observations of cosmic-ray antiprotons at low energies.

The balloon portion of this experiment was supported by NASA under grant NGR-30-002-052. The authors wish to thank Jim Kish for his support in preparing and flying the balloon-borne telescope. The *Voyager* data analysis was supported by a Caltech sucontract CIT-3 44-453800 under the auspices of R. E. Vogt. The authors wish to thank Dr. Frank McDonald at GSFC for providing the data tapes used in the *Voyager* analysis.

REFERENCES

Badhwar, G. D., Deney, C. L., Dennis, B. R., and Kaplan, M. F. 1967, *Phys. Rev.*, **196**, 1327.
Bastian, T. S., McKibben, R. B., Pyle, K. R., and Simpson, J. A. *Proc. 16th Internat. Cosmic Ray Conf.*, **5**, 338.
Buffington, A., Schindler, S. M., and Pennypacker, C. R. 1981, *Ap. J.*, **248**, 1179.
Comstock, G. M., Hsieh, K. C., and Simpson, J. A. 1972, *Ap. J.*, **173**, 691.
Garcia-Munoz, M., Mason, G. M., and Simpson, J. A. 1975, *Ap. J.*, **202**, 265.
Gleeson, L. J. 1972, unpublished.
Gleeson, L. J., and Axford, W. I. 1968, *Ap. J.*, **154**, 1101.
Gleeson, L. J., and Urch, I. H. 1971, *Ap. Space Sci.*, **11**, 288.
Golden, R. L., Horan, S., Mauger, B. G., Badhwar, G. D., Lacy, J. L., Stephens, S. A., Daniel, R. R., and Zipse, J. E. 1979, *Phys. Rev. Letters*, **43**, 1196.
Goldstein, M. S., Fisk, L. A., and Ramaty, R. 1970, *Phys. Rev. Letters*, **25**, 832.
Hsieh, K. C. 1970, *Ap. J.*, **159**, 61.
Lezniak, J. A., and Webber, W. R. 1971, *J. Geophys. Res.*, **76**, 1605.
McDonald, F. B. 1980, unpublished.
McDonald, F. B., Lal, N., Trainor, J. H., Van Hollebeke, M. A. I., and Webber, W. R. 1977, *Ap. J.*, **216**, 930.
———. 1981, *Ap. J.*, **249**, L71.
Mewaldt, R. A., Stone, E. C., and Vogt, R. E. 1976, *Ap. J.*, **206**, 616.
Meyer, J. P. 1974, Ph.D. thesis, University of Paris.
———. 1975, *Proc. 14th Internat. Cosmic Ray Conf.*, **2**, 554.
Ormes, J. F., and Freier, P. S. 1978, *Ap. J.*, **222**, 471.
Ormes, J. F., and Webber, W. R. 1968, *J. Geophys. Res.*, **73**, 4231.
Peters, B., and Westergaard, N. 1977, *Ap. Space Sci.*, **48**, 21.
Ramadurai, S., and Biswas, S. 1974, *Ap. Space Sci.*, **30**, 187.
Ramaty, R., and Lingenfelter, R. E. 1969, *Ap. J.*, **155**, 587.
Rygg, T. A., and Earl, J. A. 1971, *J. Geophys. Res.*, **76**, 7445.
Stone, E. C., Vogt, R. E., McDonald, F. B., Teegarden, B. J., Trainor, J. H., Jokipii, J. R., and Webber, W. R. 1977, *Space Sci. Rev.*, **21**, 355.
Teegarden, B. J., von Rosenvinge, T. T., McDonald, F. B., Trainor, J. H., and Webber, W. R. 1975, *Ap. J.*, **202**, 815.
Urch, I. H., and Gleeson, L. J. 1972, *Ap. Space Sci.*, **17**, 426.
Webber, W. R., and Lockwood, J. A. 1981, *J. Geophys. Res.*, **86**, 11458.
Webber, W. R., and Schofield, N. J. 1975, *Proc. 14th Internat. Cosmic Ray Conf.*, **1**, 312.
Webber, W. R., Stone, E. C., and Vogt, R. E. 1979, *Proc. 16th Internat. Cosmic Ray Conf.*, **5**, 537.
Webber, W. R., and Yushak, S. M. 1979, *Proc. 16th Internat. Cosmic Ray Conf.*, **1**, 383.
Yushak, S. M. 1978, Ph.D. thesis, University of New Hampshire.

W. R. WEBBER: Space Science Center, DeMeritt Hall, University of New Hampshire, Durham, NH 03824

S. M. YUSHAK: 9 Northbrook Drive Apt. 902 Manchester, NH 03202